ELSEVIER

Polymer 43 (2002) 6719–6726

polymer

www.elsevier.com/locate/polymer

Topological coarsening of low-molecular-weight block copolymer ultrathin films by environmental AFM

Donovan N. Leonard[a], Richard J. Spontak[a,b,*], Steven D. Smith[c], Phillip E. Russell[a]

[a]*Department of Materials Science and Engineering, North Carolina State University, Raleigh, NC 27695, USA*
[b]*Department of Chemical Engineering, North Carolina State University, Raleigh, NC 27695, USA*
[c]*Corporate Research Division, The Procter & Gamble Company, Cincinnati, OH 45239, USA*

Received 22 July 2002; received in revised form 29 August 2002; accepted 3 September 2002

Abstract

Topological coarsening of block copolymer ultrathin films is well-understood for copolymers exhibiting intermediate or strong segregation and differing in film thickness or molecular weight at temperatures above the upper glass transition temperature (T_g), but below the order–disorder transition (T_{ODT}), of the copolymers. More recent studies suggest that the stability and topology of such films differ at temperatures above T_{ODT}. In this work, we use environmental atomic force microscopy to examine the effect of temperature on the coarsening of block copolymer ultrathin films in situ. Films measuring ca. 25 nm thick consist of a low-molecular-weight poly(styrene-*b*-isoprene) diblock copolymer for which the upper T_g and T_{ODT} in the bulk are about 42 and 70 °C, respectively. Time-resolved image sequences illustrating surface reorganization are obtained at temperatures below, above and near 70 °C. At temperatures very close to 70 °C, coarsening is found to slow markedly, by almost an order of magnitude relative to what is observed at higher and lower temperatures, suggesting that thermal factors may provide a means by which to inhibit the dewetting of block copolymer ultrathin films.

Keywords: Block copolymer; Polymer dewetting; Order–disorder transition

1. Introduction

Diblock copolymers are macromolecular surfactants that are capable of spontaneous self-organization into several ordered microphases, depending principally on molecular composition, if the constituent (A and B) sequences are sufficiently incompatible [1,2]. The degree of incompatibility (χN) is governed primarily by temperature (through the Flory–Huggins χ interaction parameter) and the number of A and B statistical units along the copolymer backbone (N). For reference, compositionally symmetric (lamellar) AB diblock copolymers in the mean-field ($N \rightarrow \infty$) limit undergo an order–disorder transition (ODT) in the melt at $\chi N \approx 10$ [2,3]. For copolymers of finite N, critical fluctuations must be considered [4]. While some copolymers exhibit upper and lower ODTs, [5] we only consider systems possessing a single ODT in this work. At constant N, the bulk ODT may be induced by an increase in temperature [6–8] (or, equivalently, a reduction in χ) or the introduction of, for example, homopolymer [9,10] or solvent [11–13] (which reduces the effective interaction between A and B blocks). Alternatively, the temperature corresponding to the ODT (T_{ODT}) can be readily lowered by decreasing N [12]. Nanostructural development in block copolymers is further complicated in ultrathin films wherein the film thickness (h) approaches the period of the individual nanodomain elements (L) comprising an ordered block copolymer morphology [14,15]. Additional free energy considerations arising from the intrinsic surface energies and elasticity/registry of the A and B blocks are responsible for nanodomains adopting a preferred orientation relative to the film surface [16–21].

Such ultrathin films may, however, become unstable and form surface patterns that are sensitive to the magnitude of h relative to L. Numerous efforts [22–29] have examined the molecular and environmental driving forces responsible for the topological coarsening of block copolymer ultrathin films and have established relationships to explain the

* Corresponding author. Address: Department of Chemical Engineering, North Carolina State University, Raleigh, NC 27695, USA. Tel.: +1-919-515-4200; fax: +1-919-515-3465.
E-mail address: rich_spontak@ncsu.edu (R.J. Spontak).

0032-3861/02/$ - see front matter
PII: S0032-3861(02)00640-7

topological features of such patterns. Conventional topologies include holes, islands and a spinodal-like pattern, depending on the coupling between short- and long-range intermolecular interactions [28]. A relatively new strategy [30–32] developed for simultaneously probing large ranges of block copolymer ultrathin film coarsening behavior employs combinatorial methods to deduce, in continuous fashion, the dependence of film topology on both material properties (N), film characteristics (h) and temperature (T). Results from this methodology have nicely demonstrated that (i) films are stable when h is a near-integral multiple of L and (ii) the characteristic dimension of the pattern (λ) scales as $N^{-3/2}$. In all these prior investigations of block copolymer ultrathin films, the copolymers have exhibited either intermediate or strong segregation, in which case $\chi N \gg 10$. To complement these studies, Green and co-workers [33,34] have probed the patterning dynamics of block copolymer ultrathin films at $T > T_{ODT}$ and report that the resultant surface topology—i.e., discrete hole/island versus spinodal—is likewise dependent on film thickness and occurs via a stage-wise mechanism.

The objective of the present work is to employ environmental atomic force microscopy (AFM) to examine the topological coarsening of a relatively low-molecular-weight diblock copolymer in situ. Time-resolved AFM images are acquired from copolymer films of nearly constant thickness with $h > L$. Temperatures accessed here lie below, above and near the bulk ODT of the copolymer.

2. Experimental

2.1. Materials

The poly(styrene-*b*-isoprene) (SI) diblock copolymer employed here was synthesized by living anionic polymerization in cyclohexane at 60 °C in the presence of *sec*-butyllithium. Its number-average molecular weight and polydispersity index from GPC were 14,000 and 1.01, respectively, and its composition from ^{1}H NMR was 50 wt% S. Electron microscopy and small-angle scattering of compositionally identical copolymers of comparable molecular weight previously confirmed [12] the existence of a microphase-separated morphology composed of alternating S and I lamellae with $L = 16 \pm 1$ nm after annealing at 90 °C under vacuum (to promote equilibration). Differential scanning calorimetry of the present copolymer revealed two glass transition temperatures (T_gs), a lower one at -51 °C corresponding to the I lamellae and an upper one at 42 °C due to the presence of S lamellae. Dynamic melt rheology revealed an abrupt reduction in the dynamic storage modulus over the range $69 \leq T(°C) \leq 74$, in which case T_{ODT} (at the onset) is taken as 70 ± 1 °C. Reagent-grade toluene was purchased from Aldrich Chemicals (Milwaukee, WI) and used as-received.

2.2. Methods

The copolymer was dissolved in toluene to form a 0.5% (w/v) solution, which was subsequently spun-cast at 1500 rpm for 45 s onto Si wafers. Microelectronic-grade Si(100) wafers measuring 10 cm in diameter and 340–350 mm in thickness were cleaved into quarters. These pieces were initially cleaned in methanol, rinsed in deionized water and dried under a dry N_2 stream. They were then subjected to a second cleaning sequence in which the pieces were exposed to acetone, deionized water and dry N_2. The native oxide present on the surfaces of the Si wafers was not removed. As-spun thin films were placed under vacuum at ambient temperature for 3 h to remove residual solvent and analyzed by AFM within a couple of hours of storage under dark conditions in air. Note that the films were not annealed to promote chain relaxation or equilibration, in which case the initially cast films are anticipated to be highly phase-mixed.

Atomic force microscopy of the cleaned Si wafers with and without copolymer was performed in air (~55% humidity) with a JEOL-4200 instrument, operated in intermittent contact (IC) mode and equipped with a heating/cooling stage. Imaging was conducted with silicon tips (Olympus OMCL-AC120-TS and Nanoprobe TESP) having resonant frequencies between 260 and 330 kHz. The amplitude, scan rate and gain values were kept relatively constant for each specimen sequence, but differed slightly from specimen to specimen, to ensure artifact-free images (no discernible damage to the film surfaces was inflicted after several hours of continuous use). Images were collected in situ at a single scan position at temperatures ranging between 55 and 110 °C. The time for the heating stage to reach a predetermined temperature ranged from 30 s at $T < 80$ °C to 90 s at $T > 80$ °C. The total scan time required to record each AFM height image, measuring 10 μm × 10 μm, was 45 s. Resultant images were processed and analyzed by the Photoshop software package (Adobe) with plug-in modules from the Image Processing Tool Kit (Reindeer Games).

3. Results and discussion

The root-mean-square roughness (R) of the cleaned Si wafers is determined to be about 0.20 nm over a 100 μm^2 area. Addition of the copolymer film increases R to 0.78 nm. Pinholes and other film defects, as discerned by AFM, are evident in these films. Areas employed in the annealing experiments reported herein possess a relatively low defect density. Film thicknesses have been determined from bearing analyses, in which a sharp metal razor blade is used to scratch a copolymer film but not the underlying Si substrate. We have chosen this approach, rather than one in which the AFM tip is used for the same purpose [35], to avoid damaging the tip. Three scratches are made per film,

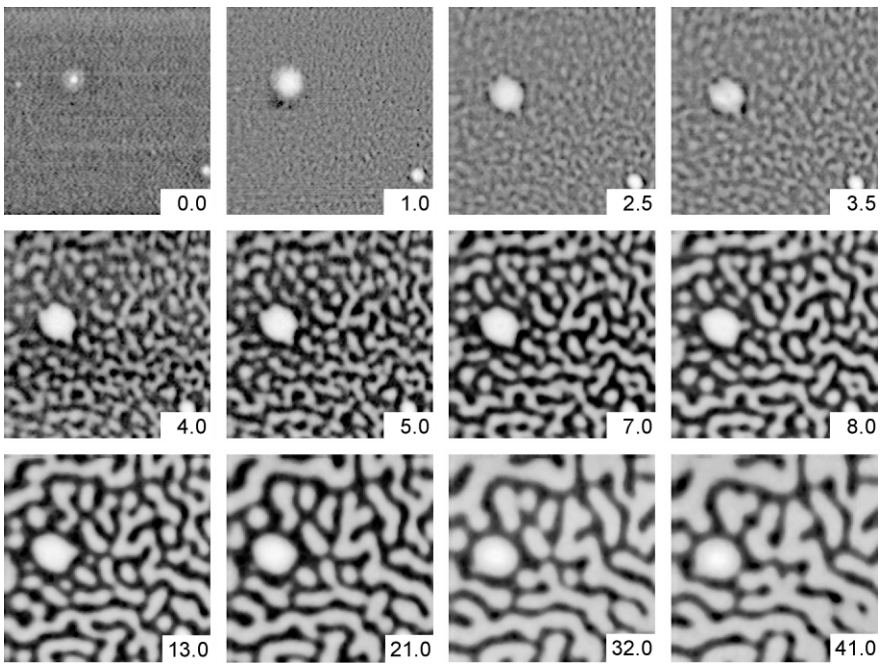

Fig. 1. Time sequence of AFM images obtained in situ from a spun-cast SI copolymer ultrathin film annealed at 55 °C. The time (in min) is displayed in each frame, which measures 10 μm × 10 μm. The image grayscale level reflects the film height (lighter levels correspond to greater height).

and the difference in height between each trench and the surrounding area (excluding the pile-up alongside each trench) is used to ascertain the film thickness. Film thicknesses determined in this fashion consistently range between 23 and 26 nm (with the average being 25 nm). This observed variation in film thickness may represent actual differences in film characteristics and/or reflect the different AFM tips used here, since the tips are expected to differ slightly in radius and some tip-specimen convolution may occur (due to the similarity in size scale). Since the average film thickness measured here is about 1.5L, topological evolution is expected.

The films examined here are stable over the course of a few days at ambient temperature. As detailed elsewhere [36], spontaneous dewetting of these films results in the formation of rimmed features and, after long times or high-temperature annealing, multiscale features that appear more complex than those described previously by Green and Limary [33]. The annealing experiments reported here are performed soon after the films are spun-cast and vacuum-dried (and well before spontaneous dewetting occurs). Fig. 1 shows a time-resolved sequence of AFM height images acquired from a film annealed at 55 °C, which is about 13 °C above the upper T_g (42 °C), but 15 °C below the T_{ODT} (70 °C), of this bulk SI copolymer. Recall, however, that these thermal properties are not of immediate relevance, since the copolymer molecules are highly confined in an ultrathin film and phase-mixed due to the initial casting conditions. The three defects visible in the virgin film (at 0.0 min) serve as reference markers in an otherwise featureless film. These defects grow in a matrix that coarsens with the appearance of submicron height undulations, which first become noticeable after about 2.5 min. As coarsening proceeds, the undulations, which nominally measure 15 nm ($\approx L$) high relative to the lower regions (valleys) composed of a residual copolymer layer remaining in contact with the Si substrate [36], become more distinct and begin to grow in size and coalesce. The image montage displayed in Fig. 1 reveals the progression of surface coarsening over the course of 41.0 min, whereas the AFM height images presented in Fig. 2 illustrate the effect of annealing at 55 °C for longer times: 175 ≤ t(min) ≤ 412. In this case, discrete holes are prevalent in the film (~15 nm high) and continue to coalesce with increasing annealing time. Note that some of the discrete holes in this image set shrink and eventually disappear altogether. It therefore

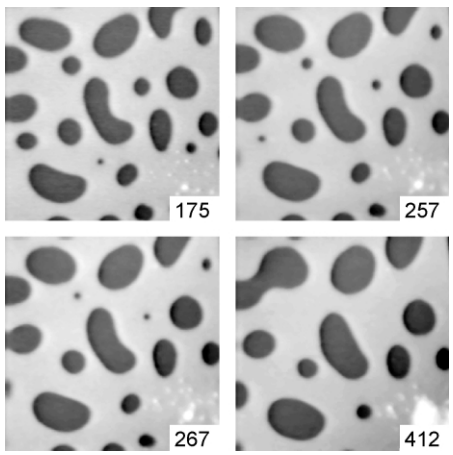

Fig. 2. Time sequence of AFM images obtained in situ from a spun-cast SI copolymer ultrathin film annealed at 55 °C for long times (identified in each frame). Details regarding these images are provided in the caption of Fig. 1.

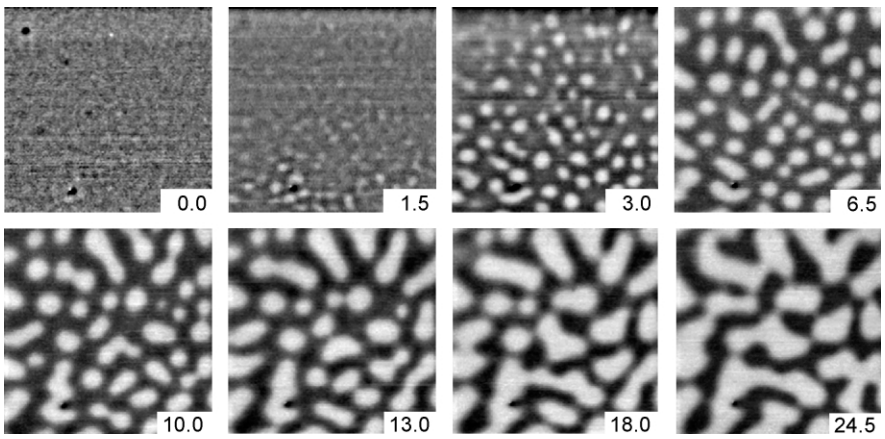

Fig. 3. Time sequence of AFM images obtained in situ from a spun-cast SI copolymer ultrathin film annealed at 93 °C. Details regarding these images are provided in the caption of Fig. 1.

follows that the pattern in Fig. 1 evolves into the hole pattern in Fig. 2 after long annealing times.

A markedly different surface topology is manifested (see Fig. 3) when the annealing temperature is increased to 93 °C. In this case, discrete islands initially measuring less than 0.5 μm in diameter and, again, ca. 15 nm in thickness relative to the surrounding valleys form after about 1.5 min. It is important to realize that the image is scanned from left to right and from top to bottom. The image acquired after 1.5 min in Fig. 3 shows no evidence of island formation at the top of the image. In the lower part of the image, however, islands become visible as they form during image acquisition. Similarly rapid topological evolution is likewise evident after 3.0 and 5.0 min. Discrete islands remain the prominent feature up to about 20 min, after which time a more semi-continuous pattern emerges as the result of island coalescence. As the time-resolved image sequence provided in Fig. 4 demonstrates, annealing one of the SI films at a higher temperature (110 °C) results in similar, but more pronounced, topological coarsening. Note that the second image in this sequence starts at 4.0 min and already displays a uniform distribution of relatively large (micron-size) islands. As the annealing time increases in this sequence, islands measuring on the order of a few microns are observed to grow at the expense of smaller ones, eventually forming a semi-continuous pattern with a characteristic length scale that approaches the size of the image (10 μm across). The height of the semi-continuous film is ~15 nm and does not vary substantially.

Fourier analysis of the images displayed in Fig. 1 would yield the characteristic wave vector (q^*), which, for a binary liquid mixture undergoing early-stage spinodal decomposition [37], is expected to scale as $t^{-1/3}$. Such scaling has been previously observed [33,34] with regard to the surface coarsening of a compositionally symmetric poly(styrene-*b*-methyl methacrylate) (SM) diblock copolymer above its ODT. Although the mechanism of spinodal dewetting shares certain common characteristics with spinodal decomposition [38], the influence of the contact surface must be considered, in which case the scaling exponent on t is predicted [39] to be slightly larger than 1/3. Unfortunately, the size ratio of surface features to AFM scan area in all the images collected during the course of this study is simply too large to permit accurate assessment of $q^*(t)$. Instead, we turn our attention to two other characteristics. The first is the area fraction of patterned surface (η), which

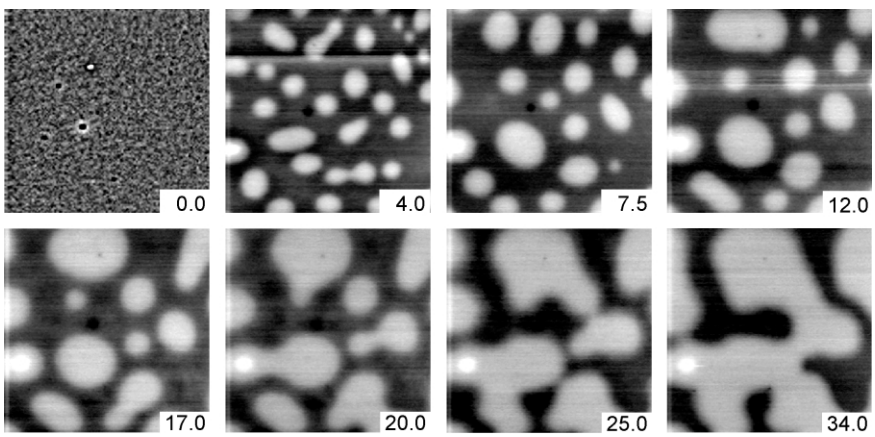

Fig. 4. Time sequence of AFM images obtained in situ from a spun-cast SI copolymer ultrathin film annealed at 110 °C. Details regarding these images are provided in the caption of Fig. 1.

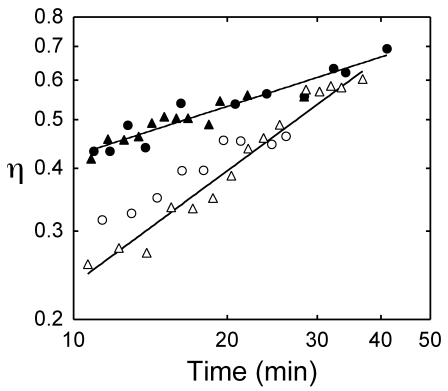

Fig. 5. Variation of patterned area fraction (η) with respect to time for SI copolymer ultrathin films heated to three different temperatures (in °C): 55 (● and ▲), 93 (○) and 110 (△). The solid lines represent power-law fits to the data at 55 and 110 °C.

represents the fraction of each image that appears light. It is presented in Fig. 5 as a function of t for two different copolymer films annealed at 55 °C (to ascertain the degree of reproducibility), as well as for the films used to generate Figs. 3 and 4 at 93 and 110 °C, respectively. Analysis of these data indicates that η scales as t^{α}, with $\alpha \approx 1/3$, at 55 °C. As the temperature is increased, the magnitude of α increases. At 93 °C, for instance, $\alpha \approx 1/2$, whereas $\alpha \approx 3/4$ at 110 °C. While these scaling exponents are extracted from limited data and may not be precise, this observation establishes that α varies with temperature, in apparent contrast to another parameter of interest here, namely, the interfacial length per unit area (P_L). Values of P_L are shown in Fig. 6 as a function of t for the three annealing temperatures included in Fig. 5. Despite their noise level, these data demonstrate that $P_L \sim t^{-\beta}$. Unfortunately, the noise evident in this figure precludes accurate assessment of β. The solid line provided in Fig. 6 corresponds to $\beta = 1/2$ and fits the data sets obtained at 55 and 93 °C reasonably well. Note that the time dependence of P_L evaluated at 110 °C cannot be discerned due to the size of the surface

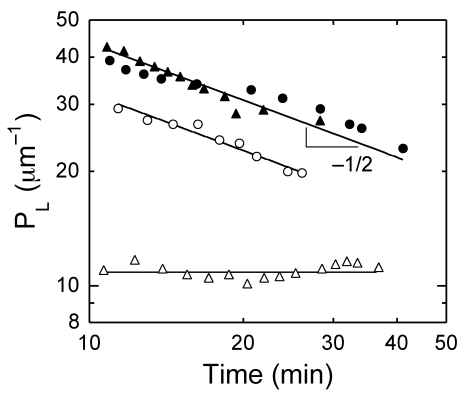

Fig. 6. The interfacial length per unit area (P_L) presented as a function of time for SI copolymer ultrathin films heated to three different temperatures (in °C): 55 (● and ▲), 93 (○) and 110 (△). The solid lines are power-law fits (with a fixed scaling exponent of $-1/2$) to the data.

features relative to the image size, in which case P_L is virtually invariant with respect to t.

In the results reported thus far, the annealing temperature has been either well below or above 70 °C. The AFM height image sequence displayed in Fig. 7 has been collected at 75 °C, which lies between the temperatures examined thus far. In this case, the height of the islands is measurably smaller (~9 nm) than the ~15 nm features evident in the images acquired at higher and lower temperatures, and no evidence of coarsening is detectable up to 10.0 min. For comparison, recall that surface coarsening is first observed at 2.5 min at 55 °C and at 1.5 min at 93 °C. Moreover, the images in Fig. 7 reveal that the *rate* of topological coarsening is considerably slower at 75 °C than at lower and higher annealing temperatures. In fact, the image at 21.0 min at 75 °C in Fig. 7 closely resembles the one corresponding to 3.0 min at 93 °C in Fig. 3. This unexpectedly slow pattern development is further explored in the time- and temperature-variable AFM images presented in Fig. 8. In this montage, we seek to demonstrate the extent to which coarsening is slowed and the reproducibility of the results reported herein. First, the film is heated to 65 °C. The temperature is then increased to and held at 72 °C for the next ~20 min without *any* discernible sign of surface coarsening. The temperature is then increased to 76 °C, in which case coarsening becomes apparent after an additional 8.0 min. This time scale is in reasonably good agreement with the results obtained under isothermal conditions at 75 °C (see Fig. 7). By further increasing the temperature to 80, 86, 90 and 103 °C (see Fig. 8 for the corresponding images), the surface pattern, initially resembling the one generated isothermally at 93 °C (see Fig. 3), evolves into a densely packed arrangement of discrete islands that continue to transform into a semi-continuous pattern. Note that the image corresponding to 78.0 min at 103 °C in Fig. 8 appears qualitatively similar to that obtained after only 24.5 min at 93 °C in Fig. 3.

The AFM images presented in Figs. 7 and 8 clearly demonstrate that the molecular process by which topological coarsening occurs is slowed substantially (by about an order of magnitude) in the vicinity of 70 °C, which surprisingly coincides with the bulk T_{ODT} of the copolymer. Unfortunately, T_{ODT} is not known for the ultrathin films (of thickness h) examined here. Although T_{ODT} has been found [40] to depend sensitively on h (scaling as $h^{-3.1}$) for SM diblock copolymers on Si supports, we do not anticipate that this $T_{ODT}(h)$ dependence applies to SI ultrathin films due to differences in surface energy and chemical affinity for Si. No corresponding data are, however, presently available to estimate T_{ODT} in analogous ultrathin films composed of SI copolymers. While ongoing experimental studies [41] of hydrogenated SI ultrathin films suggest that $T_{ODT}(h)$ does not differ much from the bulk T_{ODT}, we refrain here from drawing a relationship between T_{ODT} and the results provided in Figs. 7 and 8. Suppressed block copolymer surface coarsening has been previously realized in systems

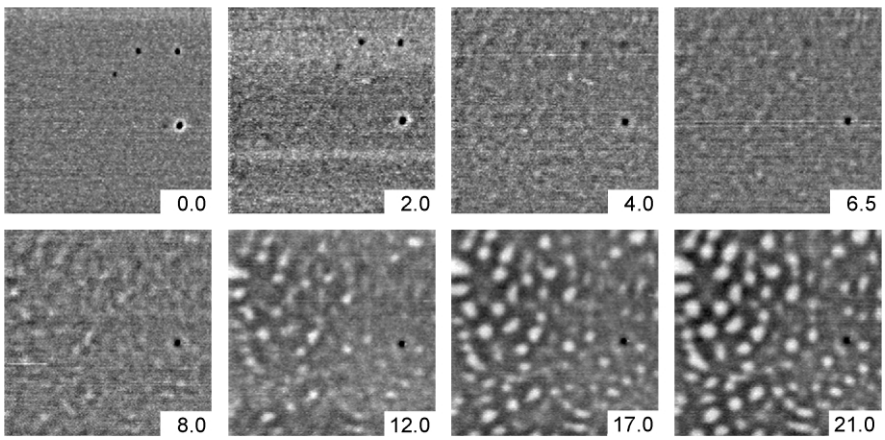

Fig. 7. Time sequence of AFM images obtained in situ from a spun-cast SI copolymer ultrathin film annealed at 75 °C. The time (in min) is displayed in each frame, which measures 10 μm × 10 μm.

to which a second component, such as a fullerene [42], dendrimer [43] or inorganic nanoparticle [44], is added to modify the surface tension at the air/polymer interface. The observation that coarsening occurs relatively quickly (on the order of a few minutes) at temperatures below and above ~70 °C, but slows substantially near 70 °C, in the present copolymer system without introducing an additive is of fundamental and applied importance, and implies that inhibited coarsening can be achieved exclusively through judicious thermal treatment.

Topological coarsening is certainly a dynamic process, requiring molecules to diffuse over relatively large length scales (greater than the gyration radius of individual copolymer chains) to form islands, holes or a spinodal pattern. One possible explanation for the anomalous behavior observed here relates to critical slowing down,

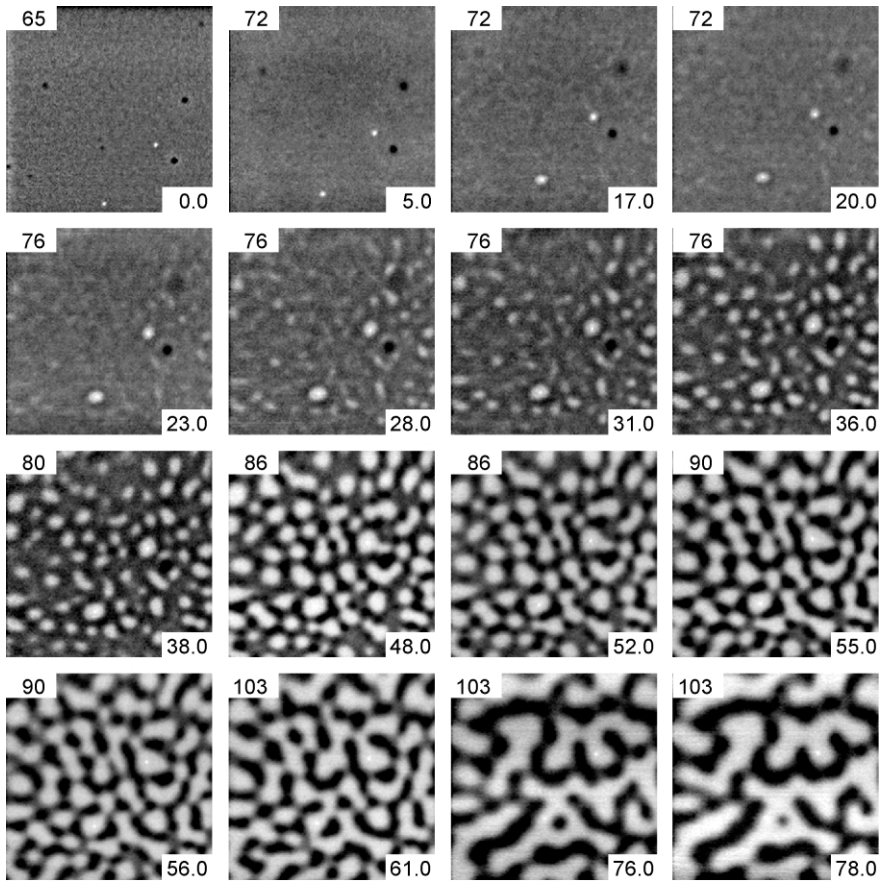

Fig. 8. Time sequence of AFM images obtained in situ from a spun-cast SI copolymer ultrathin film at varying temperatures (in °C, identified at the top left of each image) in initially close vicinity to 70 °C. Details regarding these images are provided in the caption of Fig. 7.

which requires at least one dynamic relaxation mode to become vanishingly small as a critical point is approached [45,46]. Examples of critical slowing down have been experimentally documented in macromolecular systems. Green and Doyle [47], for instance, have reported that the diffusion of polymer chains in physical blends undergoes critical slowing down. While an explanation of the experimental findings in Figs. 7 and 8 based on this phenomenon is intriguing, it must be remembered that the low-molecular-weight copolymer is, if ordered, subject to critical fluctuations as it disorders [4], in which case insufficient evidence presently exists to attribute the findings reported here to critical slowing down. Further investigation into the mechanism responsible for thermally induced suppressed coarsening of block copolymer ultrathin films is clearly warranted.

4. Conclusions

Block copolymer ultrathin films are of considerable fundamental and technological interest, but are subject to dewetting or surface coarsening due to thermodynamic instability. In this work, we have employed environmental AFM to examine the early-stage dynamics of such coarsening in situ, thereby precluding the introduction of artifacts that may arise from chain dynamics, dimensional changes or phase considerations under ex situ conditions. To achieve this objective, we have investigated the coarsening of a relatively low-molecular-weight diblock copolymer (with $T_{ODT} = 70 \pm 1$ °C) at temperatures below, above and near 70 °C. At $T < 70$ °C, the ultrathin films of this copolymer form a semi-continuous pattern that ultimately transforms into a hole pattern at long annealing times. Above 70 °C, discrete islands rapidly form and coalesce, eventually forming a semi-continuous pattern. The scaling behavior of the area fraction of patterned copolymer with respect to time is found to be sensitive to temperature, whereas that of the interfacial length per unit area is not. At temperatures at least 15 °C below and above 70 °C, the time required for surface coarsening to become discernible by AFM measures on the order of a few minutes. As 70 °C is approached, however, the time required for coarsening to be manifested increases substantially (up to ~20 min at 72 °C). Additional investigation is certainly needed to explore the generality and ramifications of thermally induced dewetting suppression, which may be exploited as a viable means to stabilize such ultrathin copolymer films *without* the use of additives.

Acknowledgements

We thank JEOL, USA for financial support, Mr C.B. Mooney of JEOL, USA for technical assistance and Drs J.F. Douglas and A.P. Smith of NIST for helpful discussions.

References

[1] Hamley IW. The physics of block copolymers. New York: Oxford University Press; 1998.
[2] Bates FS, Fredrickson GH. Phys Today 1999;52:32.
[3] Leibler L. Macromolecules 1980;13:1602.
[4] Fredrickson GH, Helfand E. J Chem Phys 1987;87:697.
[5] Russell TP, Karis TE, Gallot Y, Mayes AM. Nature 1994;368:729.
[6] Fredrickson GH, Bates FS. Annu Rev Mater Sci 1996;26:501.
[7] Floudas G, Pakula T, Velis G, Sioula S, Hadjichristidis N. J Chem Phys 1998;108:6498.
[8] Mai SM, Mingvanish W, Turner SC, Chaibundit C, Fairclough JPA, Heatley F, Matsen MW, Ryan AJ, Booth C. Macromolecules 2000;33:5124.
[9] Vaidya NY, Han CD, Kim D, Sakamoto N, Hashimoto T. Macromolecules 2001;34:222.
[10] Lee SH, Char K. ACS Symp Ser 2000;739:496.
[11] Lodge TP, Pan C, Jin X, Liu Z, Zhao J, Maurer WW, Bates FS. J Polym Sci, Part B: Polym Phys 1995;33:2289.
[12] Hong S-U, Laurer JH, Zielinski JM, Samseth J, Smith SD, Duda JL, Spontak RJ. Macromolecules 1998;31:2174.
[13] Hanley KJ, Lodge TP, Huang CI. Macromolecules 2000;33:5918.
[14] Muller M, Binder K, Albano EV. J Int Mod Phys B 2001;15:1867.
[15] Mansky P, Tsui OKC, Russell TP, Gallot Y. Macromolecules 1999;32:4832.
[16] Anastasiadis SH, Russell TP, Satija SK, Majkrzak CF. Phys Rev Lett 1989;62:1852.
[17] Coulon G, Russell TP, Deline VR, Green PF. Macromolecules 1989;22:2581.
[18] Russell TP, Coulon G, Deline VR, Miller D. Macromolecules 1989;22:4600.
[19] Collin B, Chatenay D, Coulon G, Ausserre D, Gallot Y. Macromolecules 1992;25:1621.
[20] De Rosa C, Park C, Lotz B, Wittmann JC, Fetters LJ, Thomas EL. Macromolecules 2000;33:4871.
[21] Figueiredo P, Geppert S, Brandsch R, Bar G, Thomann R, Spontak RJ, Gronski W, Samlenski R, Müller-Buschbaum P. Macromolecules 2001;34:171.
[22] Coulon G, Russell TP, Deline VR, Green PF. Macromolecules 1989;22:5677.
[23] Coulon G, Collin B, Ausserre D, Chatenay D, Russell TP. J Phys (Paris) 1990;51:2801.
[24] Coulon G, Collin B, Chatenay D, Gallot Y. J Phys II 1993;3:697.
[25] Bassereau P, Brodbreck D, Russell TP, Brown HR, Shull KR. Phys Rev Lett 1993;71:1716.
[26] Mayes AM, Russell TP, Bassereau P, Baker SM, Smith GS. Macromolecules 1994;27:749.
[27] Milner ST, Morse DC. Phys Rev E 1996;54:3793.
[28] Sharma A, Khanna R. Phys Rev Lett 1998;81:3463.
[29] Hamley IW, Hiscutt EL, Yang YW, Booth CJ. Colloid Interf Sci 1999;209:255.
[30] Meredith JC, Smith AP, Karim A, Amis EJ. Macromolecules 2000;33:9747.
[31] Smith AP, Douglas JF, Meredith JC, Amis EJ, Karim A. Phys Rev Lett 2001;87:15503.
[32] Smith AP, Douglas JF, Meredith JC, Amis EJ, Karim A. J Polym Sci, Part B: Polym Phys 2001;39:2141.
[33] Limary R, Green PF. Macromolecules 1999;32:8167.
[34] Masson JL, Limary R, Green PF. J Chem Phys 2001;114:10963.
[35] Ton-That C, Shard AG, Bradley RH. Langmuir 2000;16:2281.
[36] Leonard DN, Russell PE, Smith SD, Spontak RJ. Macromol Rapid Commun 2002;23:205.
[37] Chen H, Chakrabarti A. Phys Rev E 1997;55:5680.
[38] Vrij A. Discuss Faraday Soc 1966;42:23.
[39] Milchev A, Binder K. J Chem Phys 1997;106:1978.

[40] Menelle A, Russell TP, Anastasiadis SH, Satija SK, Majkrzak CF. Phys Rev Lett 1992;68:67.
[41] Register RA. Personal communication; 2001.
[42] Barnes KA, Karim A, Douglas JF, Nakatani AI, Gruell H, Amis EJ. Macromolecules 2000;33:4177.
[43] Barnes KA, Douglas JF, Liu D-W, Bauer B, Amis EJ, Karim A. Polym Int 2000;49:463.
[44] Mackay ME, Hong Y, Jeong M, Hong S, Russell TP, Hawker CJ, Vestberg R, Douglas JF. Langmuir 2002;18:1877.
[45] Van Hove L. Phys Rev 1954;95:1374.
[46] Landau LD, Khalatnikov IM. Dokl Akad Nauk SSSR 1954;96:469.
[47] Green PF, Doyle BL. Macromolecules 1987;20:2471.